This is the author's version of an article that has been published in IEEE Robotics and Automation Letters. Changes were made to this version by the publisher prior to publication.
The final version of record is available at http://dx.doi.org/10.1109/LRA.2017.2729663

Velocity Estimation for Ultra Lightweight Tendon Driven Series Elastic Robots

Jérôme Kirchhoff[1] and Oskar von Stryk[1]

***Abstract*—Accurate velocity estimation is an important basis for robot control, but especially challenging for highly elastically driven robots. These robots show large swing or oscillation effects if they are not damped appropriately during the performed motion. In this paper, we consider an ultra lightweight tendon driven series elastic robot arm equipped with low-resolution joint position encoders. We propose an adaptive Kalman filter for velocity estimation that is suitable for these kinds of robots with a large range of possible velocities and oscillation frequencies. Based on an analysis of the parameter characteristics of the measurement noise variance, an update rule based on the filter position error is developed that is easy to adjust for use with different sensors. Evaluation of the filter both in simulation and in robot experiments shows a smooth and accurate performance, well suited for control purposes.**

***Index Terms*—Biologically-Inspired Robots, Compliant Joint/Mechanism, Physical Human-Robot Interaction**

I. Introduction

SAFE human-robot interaction and robots working in the vicinity of humans significantly gained importance in the industrial automation in the past years. This can be seen from the growing range of different robots on the market, specifically designed for such tasks. Besides sensor driven approaches (e.g. joint torque sensors, proximity sensors, or camera based workspace observation) also mechanical approaches (e.g. cushioning, joint elasticities, and lightweight structures) can be used to benefit safe collaboration.

One challenge for joint elastic robots is to reduce or even eliminate undesired swinging or oscillating motions. A damped motion would enable higher precision and increase the acceptance of such robots because safety and performance have to be in the right balance. In order to damp oscillations in a robot controller, an accurate velocity estimation is crucial. But velocity estimation is not only related to control issues. Also, observer based methods, e.g. for friction estimation, joint stiffness estimation or collision detection, need accurate velocity estimations.

In the last decades, several velocity estimation approaches for different sensors have been developed based on numerical or statistical principles (see Section II). The applicability of these approaches highly depends on the considered robotic system. Because of the lightweight structure and small size, robots for safe human-robot interaction cannot always be equipped with high-resolution position sensors. Moreover, for joint elastic systems, the application relevant range of possible velocities and oscillations can be very large. Thus, the adaptability of the desired velocity estimation method has to be appropriate. Further, the produced velocity estimation should be smooth and without a large time delay, to avoid instabilities if used for robot control.

The main contribution of this paper is the optimization based analysis of the kinematic Kalman filter's measurement noise variance regarding velocity estimation, that revealed basic properties for optimal filter performance, and on this basis, the development of a novel measurement noise variance update rule. The introduced method has been compared with a velocity estimation filter showing the best performance, according to the filter comparison of [1]. The filter performance is evaluated in simulation experiments and based on data of an ultra lightweight tendon driven series elastic robot arm (see Fig. 1). During the experiments, the proposed filter approach shows a higher adaptability to different filter scenarios than the state-of-the-art filter. Furthermore, it is simple to adjust for use on different sensors. The accurate performance proves that the presented approach is suitable for the new class of highly elastic robots.

The paper is organized as follows. Section II gives an overview of commonly used filter approaches for velocity estimation. An optimization based analysis of the measurement noise variance Kalman filter parameter is shown in Section III. A novel update rule is introduced in Section IV. The experimental filter evaluations are described in Section V. Section VI summarizes all aspects discussed in this work.

II. Related Work

In order to estimate the velocity from time-discrete data provided by a position encoder, one can choose between many well-studied approaches. If position encoders with finite resolution are used to estimate velocity or even acceleration, two categories of data recording have to be distinguished: encoder-driven and clock-driven [2]. Encoder-driven means, that the clock reading is performed on every encoder pulse, whereas in clock-driven approaches the encoder position is recorded at fixed time intervals.

One basic approach for velocity estimation is to use a Euler-based method that computes the finite differences [3] from sampled position data. As stated in [2], the velocity resolution (encoder resolution divided by sampling time) and thus the estimation accuracy gets unacceptable at short sampling times

Manuscript received: February, 15, 2017; Revised May, 22, 2017; Accepted July, 1, 2017.

This paper was recommended for publication by Editor Kevin Lynch upon evaluation of the Associate Editor and Reviewers' comments.

[1]The authors are with the Simulation, Optimization and Robotics Group, Department of Computer Science, Technische Universität Darmstadt, Germany [kirchhoff,stryk]@sim.tu-darmstadt.de

Digital Object Identifier (DOI): see top of this page.

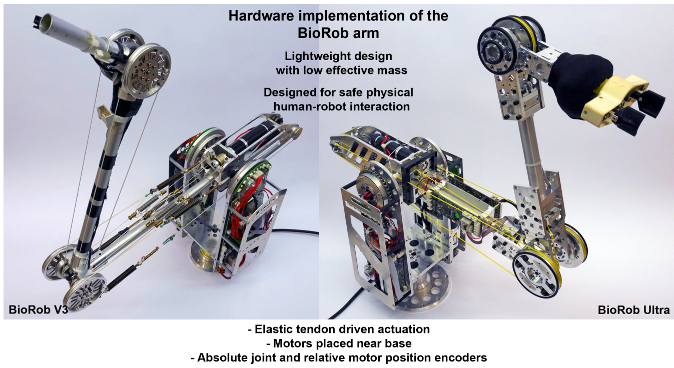

Figure 1. Hardware implementation of the BioRob arm with four elastically actuated joints. BioRob Ultra (right) is an evolution of the BioRob V3 (left).

(which is a common case in robotics), especially if the velocity is below the resulting velocity resolution. In this case, the estimation result can be improved according to the approach proposed in [4] for incremental encoders, that varies the skipped encoder positions before computing backward differences based on the maximum encoder accuracy. Such adaptive windowing techniques have also been proposed in [5] and [6]. Velocity and acceleration estimation from the pulse train of accurate optical encoders has been proposed in [7] and [8]. Another approach to reducing noise of the finite difference result is to subsequently low-pass filter the result [6], which introduces a certain time delay according to the selected cut-off frequency. Alternatively, the finite differences can be computed not on every acquired encoder position data, but only if the encoder position data changes for at least a minimum value, a so called encoder event [9].

Another possibility to create a velocity estimation is to fit a polynomial through a number of past positions [3] or encoder events [9]. The challenge using this approach is to find the appropriate polynomial order and number of passed samples.

Since estimating velocity from uncertain position information can be interpreted as state estimation, Kalman filtering [10] can be applied to this problem. The Kalman filter implements a Bayes filter for prediction of linear Gaussian systems [11]. It consists of a state prediction step based on a state transition probability and a correction step. A Kalman filter for optical shaft encoders based on a combination of encoder-driven and clock-driven acquired encoder data has been proposed in [2] using a third order process model. Based on the pulse train of optical encoders a single dimensional Kalman filter with adaptive noise variance is used in [12] to compute velocity and acceleration estimations. One advantage of the Kalman filter is that it can be used for sensor fusion. This has been done in [13] to estimate the joint state of an industrial robot equipped with an accelerometer for robot end-effector sensing.

The major velocity estimation approaches that can be used on digital position data have been compared in detail in [1]. This includes finite differences with subsequent filtering or computed from encoder events, polynomial fitting, Kalman filter estimation, and sliding mode differentiation approaches [14]. In the analyzed velocity range, the Kalman filter approach with a third order model with adaptive measurement variance provided the best results.

On ultra lightweight robots with elastic joints, optical encoders with high accuracy are typically too large and heavy to be used. Thus, a velocity estimation approach is needed, that can handle low-resolution position data that contains additional noise besides quantization. The filter performance at oscillations caused by the elastic drive train is of special interest. The adaptive Kalman filter velocity estimation approach proposed in this paper is developed based on clock-driven acquired position data. Since the experimental environment in [1] also consists of low resolution encoders with clock-driven data, evaluated on different oscillating motions, our approach is compared to the best in [1].

The proposed method only uses a kinematic process model, which keeps the computational effort low and enables to implement it on low-level controllers. Since the computational effort for integrating dynamics knowledge is high, especially for dynamic decoupled drive trains with typically no joint torque measurements, an alternative solution is preferred here.

III. Velocity Estimation Analysis

For using a Kalman filter for velocity estimation in the environment of elastically driven robots, one first has to choose the appropriate system model. Afterward, it is possible to investigate the filter performance in an ideal world with no sensor noise and known ground truth signal. Using this information, it is further possible to optimize the filter's parameters to discover the correlation between the parameters and the desired filter behavior. This is described in the following subsections.

A. Kalman Filtering

Using a Kalman filter is a common technique to estimate the state of a system from uncertain information and was first published in 1960 [10]. The Kalman filter produces a state estimation that minimizes the mean squared estimation error based on a given observation sequence [11]. Its time-discrete version estimates the state based on a linear stochastic difference equation [15]:

$$\begin{aligned} \boldsymbol{x}_k &= \boldsymbol{A}\boldsymbol{x}_{k-1} + \boldsymbol{B}\boldsymbol{u}_k + \boldsymbol{w}_{k-1}, \\ \boldsymbol{z}_k &= \boldsymbol{H}\boldsymbol{x}_k + \boldsymbol{v}_k, \end{aligned}$$

with the state vector $\boldsymbol{x} \in \mathbb{R}^n$, the state transition matrix $\boldsymbol{A} \in \mathbb{R}^{n\times n}$, the matrix $\boldsymbol{B} \in \mathbb{R}^{n\times l}$ that relates the control input vector $\boldsymbol{u} \in \mathbb{R}^l$ to the state, the matrix $\boldsymbol{H} \in \mathbb{R}^{m\times n}$ that relates the state to the measurement $\boldsymbol{z} \in \mathbb{R}^m$ and the random variables $\boldsymbol{w}$ and $\boldsymbol{v}$ that represent the process and measurement noise respectively.

The system state is estimated iteratively from one time step to the next using the following equations ([15]) for the prediction (Time-Update):

$$\hat{\boldsymbol{x}}_k^- = \boldsymbol{A}\hat{\boldsymbol{x}}_{k-1} + \boldsymbol{B}\boldsymbol{u}_k \qquad \boldsymbol{P}_k^- = \boldsymbol{A}\boldsymbol{P}_{k-1}\boldsymbol{A}^T + \boldsymbol{Q}$$

with predicted state vector $\hat{\boldsymbol{x}}_k^-$ and estimation covariance matrix $\boldsymbol{P}_k^-$. For the correction (Measurement-Update):

$$\boldsymbol{K}_k = \boldsymbol{P}_k^- \boldsymbol{H}^T \left(\boldsymbol{H} \boldsymbol{P}_k^- \boldsymbol{H}^T + \boldsymbol{R} \right)^{-1}$$

$$\hat{\boldsymbol{x}}_k = \hat{\boldsymbol{x}}_k^- + \boldsymbol{K}_k \left(\boldsymbol{z}_k - \boldsymbol{H} \hat{\boldsymbol{x}}_k^- \right) \qquad \boldsymbol{P}_k = \left(\boldsymbol{I} - \boldsymbol{K}_k \boldsymbol{H} \right) \boldsymbol{P}_k^-$$

where $\boldsymbol{K}_k$ is the Kalman gain that minimizes the estimated error covariance, the corrected state estimation $\hat{\boldsymbol{x}}_k$, and error covariance matrix $\boldsymbol{P}_k$. The matrix $\boldsymbol{Q}$ represents the process noise covariance and $\boldsymbol{R}$ represents the measurement noise variance.

In order to estimate the system state, one can use various models according to the considered filter problem, e.g. a third order kinematic model [1]. Since especially for elastic robots with possible human-robot interaction, sudden position changes can occur, a kinematic model for highly maneuvering targets with constant jerk should be regarded as presented in [16]:

$$\boldsymbol{A} = \begin{bmatrix} 1 & T & T^2/2 & T^3/6 \\ 0 & 1 & T & T^2/2 \\ 0 & 0 & 1 & T \\ 0 & 0 & 0 & 1 \end{bmatrix},$$

$$\boldsymbol{Q} = \sigma^2 \begin{bmatrix} T^7/252 & T^6/72 & T^5/30 & T^4/24 \\ T^6/72 & T^5/20 & T^4/8 & T^3/6 \\ T^5/30 & T^4/8 & T^3/3 & T^2/2 \\ T^4/24 & T^3/6 & T^2/2 & T \end{bmatrix},$$

with σ^2 the system process variance and the system state vector $\boldsymbol{x} = (q, \dot{q}, \ddot{q}, \dddot{q})^T$ containing the position q, the velocity $\dot{q}$, the acceleration $\ddot{q}$ and the jerk $\dddot{q}$ of the system. In the application presented here, this represents the state of one elastic robot joint. Using this model $\boldsymbol{H} = (1, 0, 0, 0)^T$ and $\boldsymbol{R}$ reduces to a scalar R.

B. Optimized Filter Parameter Performance

An appropriate velocity estimation has to perform well within a large frequency bandwidth. Besides the different frequencies a robot can move with, the maximum velocity can also vary in a wide range. Thus, the optimal filter settings are investigated during simulation experiments with increasing position signal frequencies and amplitudes. To simulate the real world scenario, where position changes are measured via an digital encoder with limited resolution, the position signal q is quantized into a series of discrete position values q_m:

$$q_m = \left\lfloor \frac{q}{\left(\frac{2\pi}{N}\right)} \right\rfloor \cdot \left(\frac{2\pi}{N}\right),$$

with the position signal q, the resulting measured position signal q_m and the encoder ticks per rotation N.

The objective function used to evaluate the filter performance computes the error between the estimated system state $\hat{\boldsymbol{x}}$ and the real state $\boldsymbol{x}$. Here, the root mean square error is computed individually for the position, velocity and acceleration and then added together:

$$\min_{R \in \mathbb{R}} \sqrt{\frac{\sum_{i=1}^{n} (\epsilon_{q_i})^2}{n}} + \sqrt{\frac{\sum_{i=1}^{n} (\epsilon_{\dot{q}_i})^2}{n}} + \sqrt{\frac{\sum_{i=1}^{n} (\epsilon_{\ddot{q}_i})^2}{n}}, \quad (1)$$

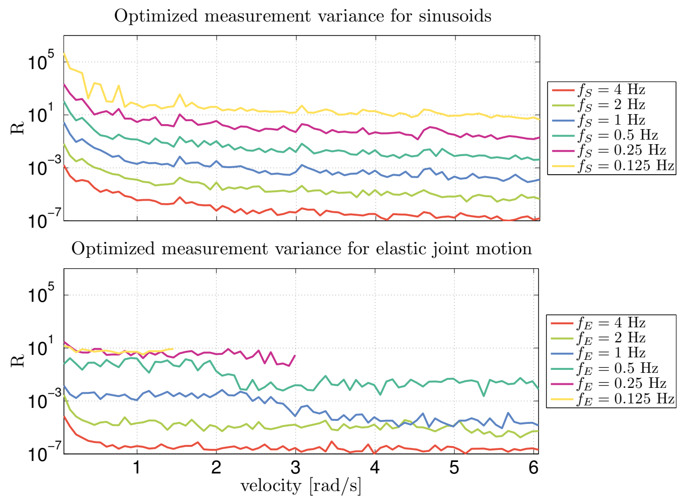

Figure 2. Result of measurement variance optimization for a kinematic Kalman filter according to the objective function (1). The optimization has been performed on a sinusoidal position signal with various frequencies and velocities. Assuming a 12Bit encoder ($N = 2^{12}$) the velocities changed between $\dot{q}_{max} = 0.001 \cdot \Delta v$ rad/s and $\dot{q}_{max} = 4.001 \cdot \Delta v$ rad/s in 0.05 rad/s steps, with a position sampling time $T = 1ms$.

with the position error $\epsilon_{q_i} = \hat{q}_i - q_i$, the velocity error $\epsilon_{\dot{q}_i} = \hat{\dot{q}}_i - \dot{q}_i$, the acceleration error $\epsilon_{\ddot{q}_i} = \hat{\ddot{q}}_i - \ddot{q}_i$ and the number of samples n. Since the velocity and acceleration deviations are typically higher than the position deviations, these have a larger influence on the optimization criterion, which results in a smoother filter result. During optimization, only the measurement noise variance R is optimized, whereas the process covariance matrix $\boldsymbol{Q}$ is kept constant.

For optimization, the MATLAB Optimization Toolbox is used with the *fmincon* algorithm, suitable for minimization of nonlinear functions. The values of R are constrained to the range of $[10^{-15}, 10^{15}]$. The optimization procedure is performed for different position signal frequencies. For each frequency, the maximum velocity amplitude and, thus, the maximum acceleration amplitude are varied from a slow to a fast motion. The maximum velocity value $\dot{q}_{max} = \alpha \Delta_v$ is computed according to the velocity resolution Δ_v of the encoder for varying $\alpha \in \mathbb{R}$. The velocity resolution is computed according to $\Delta_v = (2\pi/N)/T$ with the encoder ticks per rotation N and sampling time T. Using these equations, the signals for a chosen frequency f can be obtained from:

$$\omega = 2\pi f \qquad \bar{q} = \dot{q}_{max}/\omega \qquad q = \bar{q} \cdot \sin(\omega t) \quad (2)$$

$$\dot{q} = \omega \bar{q} \cdot \cos(\omega t) \quad \ddot{q} = -\omega^2 \bar{q} \cdot \cos(\omega t) \quad (3)$$

The optimization has been performed with the frequencies $f = 4, 2, 1, 0.5, 0.25, 0.125$ Hz and within each frequency with a velocity scaling factor between $\alpha = 0.001$ and $\alpha = 4.001$ with factor steps of 0.05. The resulting values of the optimized measurement variances R with process model variance $\sigma^2 = 10^8$ assuming a 12 Bit encoder and a third order model are depicted in Fig. 2 (top). The R-axis is plotted in logarithmic scale. Three observations with respect to the measurement variance R can be made from this analysis:

- R decreases exponentially with increasing velocity

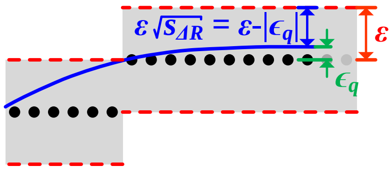

Figure 3. Visualization of quantities used in update rule for measurement variance R, with accuracy region ε (gray regions with red dashed border), position estimation error ϵ_q and update step size factor $s_{\Delta R}$. The measured positions are represented by the black dots, the filter position estimation by the blue line.

- R depends on velocity and frequency
- R is exponentially related to changing frequencies

The signal produced by a real robotic system especially with elastic joints will not be perfectly sinusoidal and superimposed by multiple frequencies. Repeating the optimization based on position data acquired from controlling sinusoidal motions with an elastic joint results in the variance values shown in Fig. 2 (bottom). Here, one can observe that the variance values drop even faster to the final value and also tend to reach a lower value if the signal additionally contains higher frequencies as the case for $f_E = 1, 0.25, 0.125$ Hz. This seems reasonable in general, since the filter has to be reactive for these additional frequencies. Because of the joint position limits, values for $f_E = 0.25, 0.125$ Hz are only available for maximum $\alpha = 2.0, 1.0$ respectively. Repeating both experiments with an order four model resulted in very similar results.

IV. Measurement Noise Variance Update Rule

As shown in the Section III-B, the choice of an appropriate measurement variance R depends on the current velocity and frequency. This has to be taken into account to achieve an optimized filter performance for velocity estimation.

A filter for velocity estimation based on position measurements needs to fulfill the following criteria:

- The filter result has to be mostly smooth.
- The velocity estimation delay has to be small.
- The filter has to be reactive within a large bandwidth.
- The filter has to be easily adjustable.

In order to fulfill the first criterion, R should be chosen as large as possible to achieve an appropriate smooth signal without a large filter delay. To keep the filter reactive to velocity changes, R should be decreased if the filter cannot follow the measured position signal.

The proposed filter adjustment rule is based on enlarging or shrinking the current value of R, according to the observations made in the previous section. This is realized by defining an accuracy region ε around the measured position. As long as the position estimation stays within this region, R is increased, otherwise it is decreased:

$$R = \exp(\log(R) + \Delta R \cdot s_{\Delta R}), \tag{4}$$

with the update step size ΔR and scaling factor $s_{\Delta R}$. As observed in the optimization experiments (see Fig. 2), R is exponentially related to changing frequencies. Thus, before updating R with an update step size having the same scale for all frequencies, its current value is logarithmized. The update rule in (4) is inspired by the gradient descent method with variable step size. Transferred to the scaling of R, the distance between the estimated position and the accuracy region border ε determines scaling of the update step size ΔR, with ΔR being a user-defined constant value determining the reactiveness of the update rule. If the estimation is within the accuracy region and far away from the border, R is increased (smoother filtering). If the estimation error approaches the border, the update step $\Delta R \cdot s_{\Delta R}$ should get smaller to prevent overshooting. In the remaining case, where the estimation error is larger than the accuracy region, R must be decreased to guarantee an accurate filter result. The step size scaling factor $s_{\Delta R}$ is calculated by

$$s_{\Delta R} = ((\varepsilon - |\epsilon_q|)/\varepsilon)^2, \tag{5}$$

with the position estimation error $\epsilon_q = \hat{q} - q$, where $\hat{q}$ the estimated and q the measured position, and the user-defined accuracy range ε. The meaning of the variables are depicted in Fig. 3. The scaling factor $s_{\Delta R}$ increases quadratically with the distance of the position signal from the accuracy border. To regard the update direction, the sign of $s_{\Delta R}$ has to be set negative in case $|\epsilon_q| > \varepsilon$.

Since position encoders can produce noisy signals (additional to the quantization noise), it should be possible to adjust the filter according to this behavior. For this purpose, we define a heuristic to compute ε. If a position variation in the sensor position signal can be observed while the joint is in rest or slowly moving, one can use the number of position variation resolution ticks n_n (or noise factor), to approximate the noise limits similar to an estimation of the 3σ interval that covers 99.7% of the noise, in the heuristic:

$$\varepsilon = \max(0.5, n_n \cdot 0.5) \cdot 2\pi/N.$$

This heuristic assumes normal distributed noise and defines the accuracy region as half of the position variation region, with at least one half of the sensor resolution. One is free to reduce this region further, but this will result in a more noisy filter result.

Since the update rule modifies R without limitations, this has to be done afterwards. Based on the optimization results (see Fig. 2) we set the limits to a range of $[10^{-20}, 10^{20}]$. Further, the scaling factor $s_{\Delta R}$ also needs to be limited as described in Section V-A.

V. Experimental Evaluation

In [1], an adaptive Kalman filter with a third order process model is proposed for velocity estimation, that outperforms commonly used approaches in a sophisticated comparison, showing less filter errors according different performance indices for a broader frequency bandwidth. This makes it very suitable for use with elastic joint robots, where velocity estimation has to be performed on position signals typically containing a broad spectrum of velocities and oscillation frequencies, and is, thus, used as reference filter for the proposed approach in this work. As performance measures

This is the author's version of an article that has been published in IEEE Robotics and Automation Letters. Changes were made to this version by the publisher prior to publication.
The final version of record is available at http://dx.doi.org/10.1109/LRA.2017.2729663

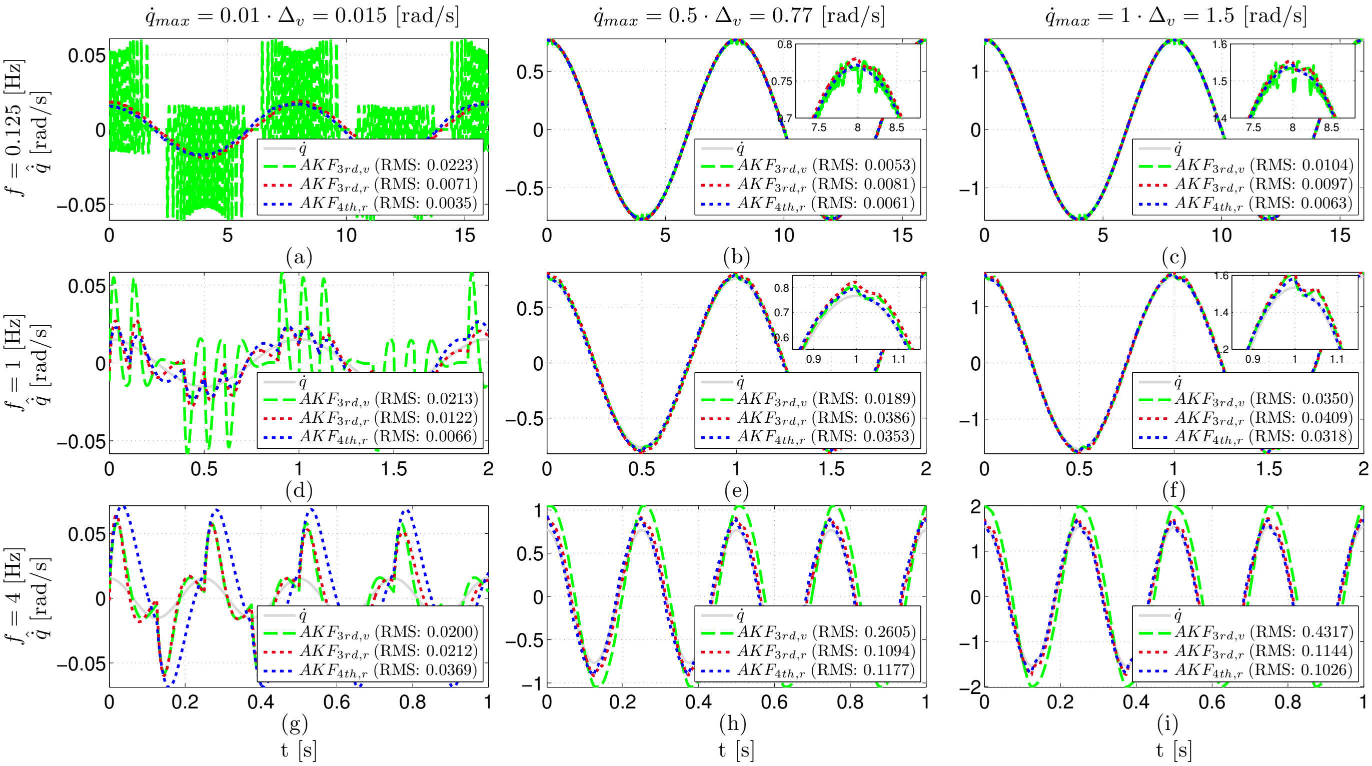

Figure 4. Filter performance evaluated on sinusoidal motions with frequencies $f = 0.125, 1.0, 4.0$ Hz (rows) and maximum velocity amplitudes $\dot{q}_{max} = s_v \Delta_v$ with $s_v = 0.01, 0.5, 1.0$ (columns). The gray solid lines represents the reference velocity signal $\dot{q}$, the green dashed lines the adaptive Kalman filter based on velocity estimation $AKF_{3rd,v}$ and the dotted red and blue line the proposed adaptive Kalman filter $AKF_{3rd,r}$ and $AKF_{4th,r}$ respectively.

the root mean square ϵ_{RMS}, the absolute maximum relative ϵ_{MAX} and average relative ϵ_{AVG} errors are used.

The adaptive Kalman filter in [1] is based on the knowledge that the noise caused by encoder quantization is significant at low and neglectable at high speeds [17]. Regarding this, the measurement noise variance R_v (subscript v denotes the velocity dependancy) can be recomputed using the current velocity estimation according to

$$R_v = 10 R_b \left(1 + \hat{\dot{q}}\right)^{-1} \tag{6}$$

with the application-dependent base measurement variance R_b and the estimated velocity $\hat{\dot{q}}$. This and the proposed filter are compared first in simulation experiments to investigate the characteristic behavior and further evaluated in experiments on an elastic, tendon driven ultra lightweight robot.

A. Evaluation in Simulation Experiments

The first experiment concerns the adaptability of the filters. The filters have been evaluated on sinusoidal motions according to (2), (3) with varying frequencies $f = 0.125, 1.0, 4.0$ Hz and slow to moderate velocities according to maximum velocity amplitudes with $s_v = 0.01, 0.5, 1.0$. As filter parameters, the system noise variance $\sigma^2 = 10^8$ and the initial respectively base measurement variance $R = 10^{-1}$ and $R_b = 10^{-1}$ for the corresponding update rule has been set. The measurement variance has been taken from the optimization results (see Fig. 2 top), approximately representing the optimal value for the mean frequency and velocity in the regarded range. Concerning the update Rule (6) and the characteristics of the optimal measurement variance, adjustments of R_b would shift the optimal filter results to another frequency and velocity range.

The results of the performed experiments for the proposed Kalman filter $AKF_{3rd,r}$ and compared Kalman filter $AKF_{3rd,v}$ are shown in Fig. 4 with the performance indices listed in Table I. The filter performance at low frequency and slow velocity (Fig. 4 (a)) shows that the proposed filter produces smaller estimation errors for all indices. These results can also be observed for high frequency and medium to high velocity (Fig. 4 (h), (i)) with $AKF_{3rd,v}$ showing more overshooting and a considerable signal time delay. In the case depicted in Fig. 4 (b), (c) the ϵ_{RMS} is not sufficient to distinguish the performance. Here, ϵ_{MAX} and ϵ_{AVG} are smaller for the $AKF_{3rd,r}$ filter, thus, produce a better filter result also visualized in the close-ups. In Fig. 4 (e), (g) the compared filter $AKF_{3rd,v}$ performs better. Whereas in case Fig. 4 (f) both filters perform comparable well. For medium frequency and low velocity $AKF_{3rd,r}$ shows smaller errors except for ϵ_{MAX} indicating that the estimation error close to zero crossing is larger, but the small error ϵ_{RMS} is more relevant if looking at the large peaks produced by $AKF_{3rd,v}$. Overall, the proposed filter outperform the compared one in low frequency for the whole velocity range, mid frequency with slow velocity, and high frequency with mid and high velocity. In the remaining cases the $AKF_{3rd,v}$ performs better or

This is the author's version of an article that has been published in IEEE Robotics and Automation Letters. Changes were made to this version by the publisher prior to publication.
The final version of record is available at http://dx.doi.org/10.1109/LRA.2017.2729663

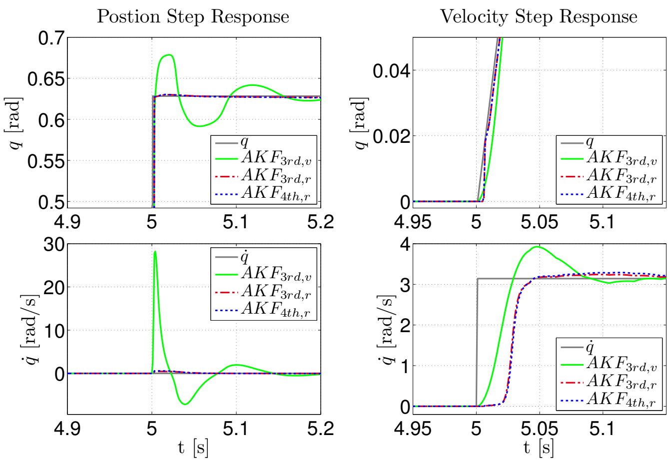

Figure 5. Step response behavior of the investigated adaptive Kalman filters for a position step of $\pi/50$ [rad] (left column) and a velocity step of $\pi/10$ [rad] (right column).

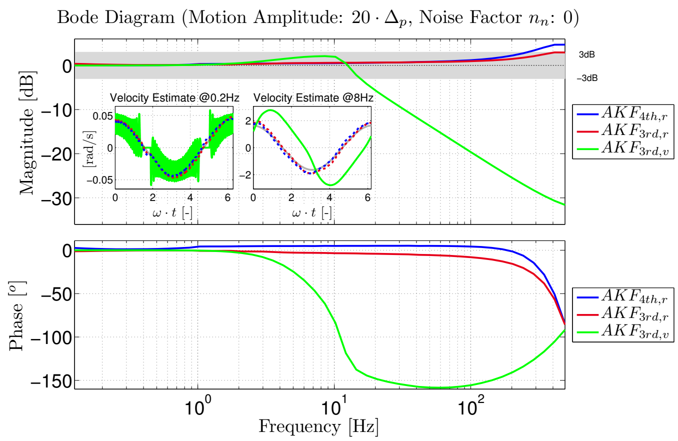

Figure 6. Bode diagram for the adaptive Kalman filters. Analyzed amplitude amplification and phase shift of velocity estimation resulting from a sinusoidal motion with amplitude of $20 \cdot \Delta_p$ sensor resolution steps. Gray area represents the 3 dB region. Detail plots show the time domain velocity estimation according to 0.2 Hz and 8 Hz motion with true velocity in gray.

equally. Adjusting R_b would shift this improved performance to another frequency range. As shown in Table I (gray values), increasing the filter's order ($AKF_{4th,r}$) mostly reduces ϵ_{RMS} compared to $AKF_{3rd,r}$ but increases the relative errors resulting from an increases phase shift.

Besides the performance evaluation in oscillation motions, another insight into to the filter properties can be gained from a step response, as shown in Fig. 5. Here, the two relevant step signals in case of velocity filtering are shown, with position measurement sampling time of $T = 1$ ms and $N = 2^{12}$ sensor ticks per turn. In the left column a step of $\pi/50$ rad is introduced in the position signal, where in the right column the velocity signal contains a step of π rad/s. In all experiments the proposed filters shows lower overshooting. Whereby, $AKF_{3rd,r}$ and $AKF_{4th,r}$ are quite reactive, since they show a small settling time of $3ms$. Considering the velocity step, $AKF_{3rd,v}$ follows the velocity signal faster but shows a larger overshoot. The step experiments further showed for the encoder with $N = 2^{12}$ ticks that the overall update value $\Delta R \cdot s_{\Delta R}$ of R should not get larger than 10. Otherwise, the filters $AKF_{3rd,r}$ and $AKF_{4th,r}$ produced a continuous oscillating velocity estimation.

The bandwidths of the filters are evaluated via a frequency analysis of a sinusoidal motion with an amplitude of a multiple of the sensor resolution. The filter result is then analyzed regarding the amplitude amplification and phase shift in comparison to the input signal using a Fourier transformation. The result is shown in Fig. 6 using a Bode diagram. The filter input signal has an amplitude of $20 \cdot \Delta_p$ (amplitude of approximately 1.75^o) using a sensor with a resolution of $N = 2^{12}$ Bit. The frequency analysis from 0.125 Hz to 480.0 Hz shows that the resonance frequency of the proposed filter update rule of $AKF_{3rd,r}$ and $AKF_{4th,r}$ is much higher than for the alternative filter $AKF_{3rd,v}$. Even for the investigated small motion, a filter performance for $AKF_{3rd,r}$ and $AKF_{4th,r}$ with low amplitude amplification and phase shift up to approx. 100.0 Hz is obtained. The detail plots for 0.2 Hz and 8.0 Hz show the time domain filter results, which is less noisy for the proposed filters especially for a low frequency (which is not immediately evident using only the Bode diagram) and has a small phase shift for mid to high frequencies. Both filters with the proposed update rule behave quiet similar in the case without noise but with the $AKF_{3rd,r}$ filter showing a smaller resonance peak.

Performing the same analysis with noise in the position signal ($n_n = 2.0$) showed that the filter performance of $AKF_{4th,r}$ still has low noise, amplitude amplification and phase shift for low frequencies and only a slightly higher amplitude amplification for high frequencies, compared to the performance with no noise. This also holds for $AKF_{3rd,r}$, except that the phase shift is increased, what makes the higher order filter more suitable in this case.

B. Evaluation in Robot Experiments

In order to investigate the filter behavior on real world data, the filters performance has been evaluated using the BioRob arm [18]. This ultra lightweight (approximately 6 kg mass) tendon driven robot is highly elastic because of the used springs. The arm is equipped with rotary position encoders on motor and joint side. Since the elasticities decouple the motor from joint actuation, a robust velocity estimation on joint side is crucial for good control performance. Due to the lightweight structure, only small and light sensors can be used. Magnetic encoders based on the Hall effect can fulfill these requirements and are used in the BioRob arm. The position values are acquired clock-driven each $T = 1$ ms according to the control frequency of 1 kHz.

The filter performance has been evaluated using experiments that covers the common scenarios, as slow to fast motions with oscillations, sudden changes of the end effector load and point to point motions (pick and place). In order to visualize the velocity resolution and noise behavior of the sensors, the finite backward differences (FD) are shown. The velocity estimation reference signals has been computed offline with a two-sided Savitzky-Golay smoother (linear polynomial with manually

This is the author's version of an article that has been published in IEEE Robotics and Automation Letters. Changes were made to this version by the publisher prior to publication.
The final version of record is available at http://dx.doi.org/10.1109/LRA.2017.2729663

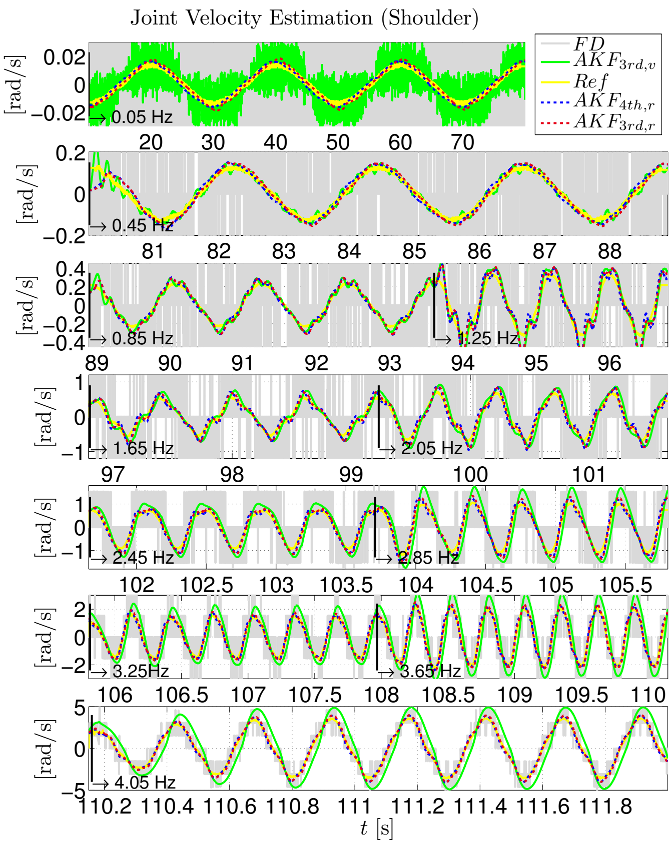

Figure 7. Filter performance of a sinusoidal motion with increasing frequencies recorded from the robot experiment with the BioRob V3 arm.

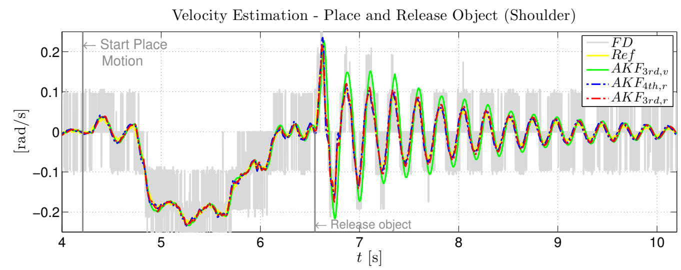

Figure 8. Velocity estimation during object (500 g) placing and releasing with the BioRob Ultra arm.

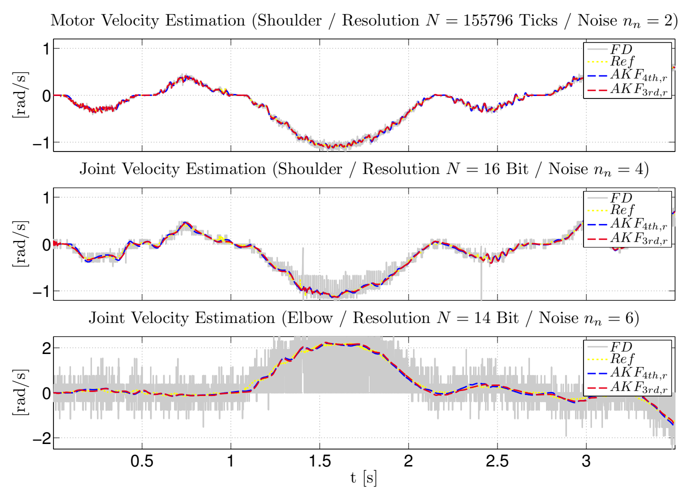

Figure 9. Velocity estimation during a Pick and Place motion with the BioRob Ultra arm in shoulder and elbow joint. The motor resolution is reflected thru the gear to the joint, creating a high resolution low noise signal.

tuned window length) that is well suited to reproduce the signal from sampled data.

In the first robot experiment, the adaptability of the filters is investigated. For this, a sinusoidal motion with an amplitude of approximately $2.5°$ and increasing frequency starting from $f = 0.05$ Hz to $f = 4.05$ Hz in 10 steps is executed on the robot, with a sensor resolution of $N = 2^{12}$ ticks per revolution. Here, a simple motor side P-Controller is used to actuate the robot. To regard noise, the base measurement variance is set to $R_b = 10^0$ and, since with the considered encoder hardware the positions varied one to two ticks with the joint in rest, the noise factor is set to $n_n = 1$. The filter results are depicted in Fig. 7 and performance measures listed in Table II. Analog to the simulation experiment, $AKF_{3rd,v}$ shows a noisy velocity estimation at low velocities and a remarkable overshoot with time delay at high velocity and frequency. According to the experimental evaluation, the proposed filters $AKF_{3rd,r}$ and $AKF_{4th,r}$ barely show noise at low speed and only little overshooting at high speed motions, resulting in overall smaller estimation errors.

Sudden changes of the end effector load can strongly alter the motion behavior of elastic systems. This has been investigated during placing and releasing an object (500 g) with the BioRob Ultra (16 Bit sensor with low noise) that causes oscillations after the place motion. The velocity estimations are shown in Fig. 8 ($R_b = 10^{-1}$, init $R = 10^{-1}$, $n_n = 1$) and the estimation errors of both phases (place motion, release object) are listed in Table III. According to the estimation errors, all filter show a rather similar performance during the place motion, whereas the proposed filter are more accurate during the oscillations.

A typical task for robots consists of part handling with a pick and place motion. This kind of motion has been performed with the BioRob Ultra arm to show the adjustability of the proposed filters. Velocity estimation has been performed on different position signals, with a separate filter for each signal. After only adaption of the sensor resolution and noise factor parameters for $AKF_{3rd,r}$ and $AKF_{4th,r}$ according to the measurement (see finite differences in Fig. 9), the filters estimated the velocities as depicted in Fig. 9 (only half a cycle shown) and with the estimation errors listed in Table IV. Even at signals with high noise, the filters produce an accurate performance, with nearly similar accuracy in a subsequently repeated second cycle.

VI. Conclusion

In this paper, the Kalman filter based velocity estimation using low-resolution encoders has been investigated for ultra lightweight tendon driven elastic robots. For this, the measurement variance characteristics regarding a wide range of signal velocities and frequencies have been analyzed. Based on these observations, a novel adaptive measurement noise variance update rule has been introduced that is easy to adjust to other

Table I
ESTIMATION ERRORS OF SIMULATED SINUSOIDAL SIGNALS ACCORDING TO FIG. 4

	Filter	$\dot{q}_{max} = 0.01\Delta_v$			$\dot{q}_{max} = 0.5\Delta_v$			$\dot{q}_{max} = 1.0\Delta_v$		
		ϵ_{RMS}	ϵ_{MAX}	ϵ_{AVG}	ϵ_{RMS}	ϵ_{MAX}	ϵ_{AVG}	ϵ_{RMS}	ϵ_{MAX}	ϵ_{AVG}
$f = 0.125$ Hz	$AKF_{3rd,v}$	0.0223	10.8689	1.8739	**0.0054**	11.076	0.0444	0.0101	16.4375	0.0395
	$AKF_{3rd,r}$	**0.0022**	**0.9554**	**0.1941**	0.0074	**1.5983**	**0.0199**	**0.0095**	**2.9077**	**0.0153**
	$AKF_{4th,r}$	0.0021↓	2.7270↑	0.2811↑	0.0051↓	5.6780↑	0.0388↑	0.0061↓	5.6363↑	0.0240↑
$f = 1.0$ Hz	$AKF_{3rd,v}$	0.0213	**4.5651**	1.9639	**0.0189**	**1.6306**	**0.0549**	**0.0335**	**2.2612**	**0.0558**
	$AKF_{3rd,r}$	**0.0066**	8.9505	**0.7019**	0.0310	2.7000	0.0896	**0.0387**	**2.2519**	**0.0576**
	$AKF_{4th,r}$	0.0058↓	7.8055↓	0.7320↑	0.0249↓	6.1141↑	0.1400↑	0.0293↓	2.7718↑	0.0743↑
$f = 4.0$ Hz	$AKF_{3rd,v}$	**0.0210**	**3.5214**	**1.6973**	0.2676	30.2556	1.4333	0.4330	25.5303	1.1989
	$AKF_{3rd,r}$	**0.0214**	17.2821	2.0267	**0.0868**	**2.7127**	**0.1914**	**0.1081**	**0.7184**	**0.1037**
	$AKF_{4th,r}$	0.0385↑	39.1094↑	5.4942↑	0.0833↓	12.0087↑	0.4702↑	0.0928↓	7.1051↑	0.2779↑

Table II
ESTIMATION ERRORS OF RECORDED MOTION ACCORDING TO FIG. 7

Filter	ϵ_{RMS}	ϵ_{MAX}	ϵ_{AVG}
$AKF_{3rd,v}$	0.2611	38.9285	0.6860
$AKF_{3rd,r}$	**0.0643**	**8.9916**	**0.2372**
$AKF_{4th,r}$	0.0688↑	11.9324↑	0.2543↑

Table III
ESTIMATION ERRORS OF RECORDED MOTION ACCORDING TO FIG. 8

Motion	Filter	ϵ_{RMS}	ϵ_{MAX}	ϵ_{AVG}
Place Object	$AKF_{3rd,v}$	0.0470	1.4721	0.3459
	$AKF_{3rd,r}$	0.0467	1.4633	0.3481
	$AKF_{4th,r}$	0.0468	1.5575	0.3441
Object Released	$AKF_{3rd,v}$	0.0533	2.4545	0.5494
	$AKF_{3rd,r}$	0.0442	1.4607	0.5028
	$AKF_{4th,r}$	0.0443	1.4793	0.5274

Table IV
ESTIMATION ERRORS OF RECORDED MOTION ACCORDING TO FIG. 9

Signal	Cycle	Filter	ϵ_{RMS}	ϵ_{MAX}	ϵ_{AVG}
$\dot{\theta}_s$	One	$AKF_{3rd,r}$	0.0176	1.1400	0.0656
		$AKF_{4th,r}$	0.0224	1.3903	0.0850
	Two	$AKF_{3rd,r}$	0.0187	1.0549	0.0650
		$AKF_{4th,r}$	0.0228	1.2256	0.0733
$\dot{q}_s$	One	$AKF_{3rd,r}$	0.0320	1.3416	0.1165
		$AKF_{4th,r}$	0.0358	1.5757	0.1268
	Two	$AKF_{3rd,r}$	0.0315	1.5378	0.1054
		$AKF_{4th,r}$	0.0339	1.5296	0.1046
$\dot{q}_e$	One	$AKF_{3rd,r}$	0.0863	3.1109	0.2823
		$AKF_{4th,r}$	0.0939	2.5239	0.2842
	Two	$AKF_{3rd,r}$	0.0873	3.3753	0.2964
		$AKF_{4th,r}$	0.0936	3.5369	0.3281

encoders. This rule uses the filter's position estimation error (residual) to decide whether the velocity estimation should be smoothed or is not accurate enough. The proposed filter has been compared to the most promising alternative based on the analysis of [1]. It has been shown in simulation and robot experiments that the new adaptive Kalman filter approach adapts better to the investigated application scenario of an ultra lightweight tendon driven elastic robots with low time delay. Furthermore, it produces a smooth and accurate velocity estimation over a wide bandwidth, which is promising with regards to using for control purposes. Additionally, the general filter concept is not limited to be used on highly elastic robots and also provides an acceleration estimation that should be investigated in further studies.

REFERENCES

[1] L. J. Puglisi, R. J. S. Pazmiño, and C. E. G. Cena, "On the velocity and acceleration estimation from discrete time-position sensors," *J. of Control Eng. and Appl. Informatics*, vol. 17, no. 3, pp. 30–40, 2015.

[2] P. Belanger, P. Dobrovolny, A. Helmy, and X. Zhang, "Estimation of angular velocity and acceleration from shaft-encoder measurements," *The Int. J. of Robotics Research*, vol. 17, no. 11, pp. 1225–1233, 1998.

[3] R. H. Brown, S. C. Schneider, and M. G. Mulligan, "Analysis of algorithms for velocity estimation from discrete position versus time data," *IEEE Trans. Ind. Electron.*, vol. 39, no. 1, pp. 11–19, Feb 1992.

[4] G. Liu, "On velocity estimation using position measurements," *IEEE American Control Conf.*, vol. 2, pp. 1115–1120, 2002.

[5] E. Kilic, O. Baser, M. Dolen, and E. Konukseven, "An enhanced adaptive windowing technique for velocity and acceleration estimation using incremental position encoders," *Int. Conf. on Signals and Electronic Systems*, pp. 61–64, 2010.

[6] F. Janabi-Sharifi, V. Hayward, and C. S. J. Chen, "Discrete-time adaptive windowing for velocity estimation," *IEEE Trans. on Control Systems Technology*, vol. 8, no. 6, pp. 1003–1009, 2000.

[7] S. H. Lee and J. B. Song, "Acceleration estimator for low-velocity and low-acceleration regions based on encoder position data," *IEEE/ASME Trans. on Mechatronics*, vol. 6, no. 1, pp. 58–64, 2001.

[8] R. Petrella, M. Tursini, L. Peretti, and M. Zigliotto, "Speed measurement algorithms for low-resolution incremental encoder equipped drives: a comparative analysis," in *Electrical Machines and Power Electronics, 2007. Int. Aegean Conf. on*, Sept 2007, pp. 780–787.

[9] R. Merry, M. van de Molengraft, and M. Steinbuch, "Velocity and acceleration estimation for optical incremental encoders," *Mechatronics*, vol. 20, no. 1, pp. 20 – 26, 2010.

[10] R. E. Kalman, "A New Approach to Linear Filtering and Prediction Problems," *Trans. of the ASME - J. of Basic Engineering*, no. 82 (Series D), pp. 35–45, 1960.

[11] H. Durrant-Whyte and T. C. Henderson, *Multisensor Data Fusion*. Berlin, Heidelberg: Springer Berlin Heidelberg, 2008, pp. 585–610.

[12] W. Shaowei and W. Shanming, "Velocity and acceleration computations by single-dimensional kalman filter with adaptive noise variance," *Electrotechn. Review*, vol. 2013, no. 02, pp. 283–287, 2012.

[13] W. Chen and M. Tomizuka, "Direct joint space state estimation in robots with multiple elastic joints," *IEEE/ASME Trans. on Mechatronics*, vol. 19, no. 2, pp. 697–706, April 2014.

[14] A. Damiano, G. L. Gatto, I. Marongiu, and A. Pisano, "Second-order sliding-mode control of dc drives," *IEEE Trans. on Ind. Electronics*, vol. 51, no. 2, pp. 364–373, April 2004.

[15] G. Welch and G. Bishop, "An introduction to the Kalman filter," in *Proc. of SIGGRAPH, Course 8*, Los Angeles, CA, USA, August 12-17 2001.

[16] K. Mehrotra and P. R. Mahapatra, "A jerk model for tracking highly maneuvering targets," *IEEE Trans. on Aerosp. and Electron. Syst.*, vol. 33, no. 4, pp. 1094–1105, Oct 1997.

[17] F. Flacco, A. De Luca, I. Sardellitti, and N. G. Tsagarakis, "Robust estimation of variable stiffness in flexible joints," in *IEEE Int. Conf. on Intelligent Robots and Systems*, 2011, pp. 4026–4033.

[18] T. Lens, J. Kirchhoff, and O. von Stryk, "Dynamic modeling of elastic tendon actuators with tendon slackening," in *IEEE/RAS Int. Conf. on Humanoid Robots*, Osaka, Japan, Nov. 29-Dec. 1 2012, pp. 779–784.